# Vortex pinning by surface geometry in superfluid helium

I. H. Neumann and R. J. Zieve
*Physics Department, University of California Davis, Davis, CA 95616, USA*
(Received 11 July 2013; revised manuscript received 9 March 2014; published 28 March 2014)

We present measurements of how a single vortex line in superfluid helium interacts with a macroscopic bump on the chamber wall. Rather than observing a unique pin location, we find that a given applied velocity field can support pinning at multiple sites along the bump, both near its apex and near its edge. We also find that a vortex can pass near or even traverse the bump itself with or without pinning, depending on its path of approach to the bump. We discuss our results in light of past computational work on vortex pinning by a hemispherical bump, as well as our own simulations that incorporate additional aspects of the experimental setup.

DOI: 10.1103/PhysRevB.89.104521 PACS number(s): 67.25.dk, 47.32.C−, 67.25.dg

Superfluid helium is in many ways a great simplification over classical fluids. It has zero viscosity, essentially zero compressibility, and zero vorticity except at isolated vortex cores each with identical fixed circulation. One advantage is that idealized hydrodynamics calculations can be compared to actual experimental results. Agreement has been found for several nontrivial experimental behaviors including precession and pinning [1,2], the speed of a vortex front [3], the distribution of vortex ring sizes emitted from superfluid turbulence [4], and details of vortex reconnections [5,6]. The calculations use the Biot-Savart law to find the velocity field from the positions of the vortices, then update the vortex positions according to this velocity field [7]. A key approximation, that the vortex core is infinitesimal, simplifies the computations substantially. In most fluids this assumption is unrealistic, but in superfluid $^4$He the core radius of 1.3 Å is indeed small enough to be ignored on typical computational length scales. Understanding this "slender vortex" situation sets the stage for modeling classical fluid motion, which can involve additional complications through changes in the size, shape, and circulation of the vortex cores.

Here we experimentally track a single vortex in superfluid helium interacting with a macroscopic bump. We compare to Schwarz's computational work for a hemispherical bump on an otherwise flat wall [7]. Schwarz uses a flow field that far from the bump is uniform and parallel to the wall. If a vortex is swept into the vicinity of the bump, then for sufficiently low applied velocity the bump captures and pins the vortex [7]. The calculation uses no explicit pinning forces; rather, a stationary configuration arises entirely because the vortex settles into an arrangement with zero net velocity along its core. For a given flow velocity, the pinned vortex terminates at a unique position on the bump, in the plane perpendicular to the flow. With increasing velocity, the pin site moves out along the bump towards the wall. Our experiments confirm that a vortex can pin at a bump, although the vortex pins less easily than expected and can exhibit multiple pin sites for the same applied velocity field.

Our data come primarily from a cylindrical cell of diameter 5.79 mm, with a large bump midway along its length. At its widest the bump has a roughly circular cross section of diameter 3.05 mm, and it protrudes 1.27 mm from the circular wall. The cell is mounted on a pumped $^3$He cryostat and filled with $^4$He through a small inlet hole [2]. A fine wire runs near the cylinder axis, in a perpendicular magnetic field of order 25 mT, as shown in the inset of Fig. 1(a). Passing a brief current pulse through the wire in the static magnetic field displaces the wire from its equilibrium position. After the pulse ends, the wire's tension causes vibrations and ultimately a return to the equilibrium position. As the wire moves through the magnetic field, we monitor the emf induced across it.

We create vortices by rotating the cryostat at low temperatures, but we make all measurements with the cryostat stationary. Vorticity trapped around all or part of the wire alters the observed vibration frequencies. We focus on the frequency splitting between the two lowest modes. The earliest measurements with a straight vibrating wire [8] confirmed that circulation is quantized in superfluid helium, since the frequency splitting expected from a single quantum of circulation was strikingly stable. However, intermediate values of the frequency splitting also occurred. These levels appear when a quantized vortex covers only a fraction of the wire and hence has a reduced effect on the vibration frequencies. The observed frequency splitting pinpoints the spot where the vortex leaves the wire. The vortex then continues through the fluid as a free vortex, with the free portion moving at the local fluid velocity. Since this motion often leads to small adjustments to the position where the vortex leaves the wire, our vibrating wire measurements can track the free vortex portion.

In our physical experiment, the driving field is the flow field of the trapped vertical vortex, which sweeps the free vortex segment around the cell. The free vortex terminates on the cell wall, and if it encounters the bump during its precession, it can pin to the bump. The observed circulation along the wire then stabilizes; the steady energy loss that we see during precession ceases, as does the oscillatory signal corresponding to the circuit of the vortex around the wire.

As a first indication that there is more than one metastable configuration for the vortex on the bump, we observe not one but *three* closely spaced stable levels. Two appear in Fig. 1. On approaching the bump, the vortex first pins with 20.7 mm of the wire's length covered by circulation, which changes to 22.0 mm after several minutes. Figure 2 includes the remaining level, at 19.6 mm. The differences between these heights are comparable to the widest radius of the bump. Thus the middle level may correspond to pinning at the apex of the bump, while the other two levels indicate pinning close to the top and bottom of the circle where the bump meets the wall.

 

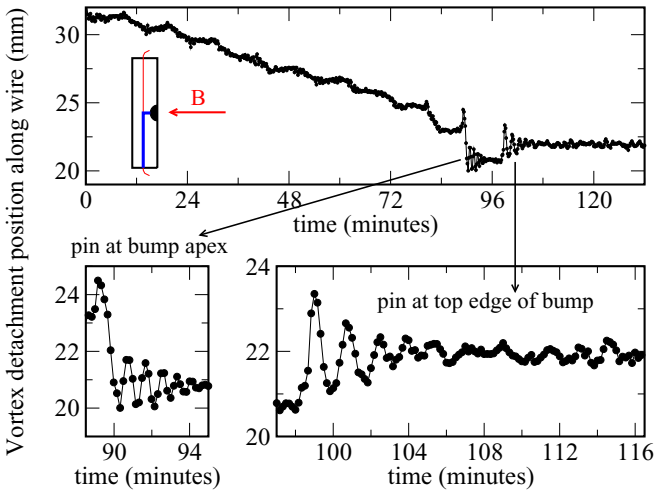


FIG. 1. (Color online) Top, inset: cell geometry, with wire stretched near cell axis, a perpendicular magnetic field used to excite and detect the wire's vibration, and a bump on the side wall. A vortex extends along the wire from the bottom of the cell to the center, then leaves the wire and terminates on the bump. Top, main: motion of the end of the vortex along the wire. Initial oscillations indicate precession of the free vortex. Pinning begins near 90 minutes. Bottom: expanded views of Kelvin waves on pinned vortices.

Kelvin waves during the pins confirm that the three levels correspond to pinning at different parts of the bump. The Kelvin waves appear as rapid oscillations superimposed on the steady circulation. Our vibrating wire itself can excite these waves, particularly when the other end of the vortex is fixed [9]. The observed oscillation frequency corresponds to the longest-wavelength mode with the vortex fixed at the cell wall and free to move vertically along the wire. (Empirically, since we observe oscillations at the Kelvin wave frequency, the vortex must not be fixed at the wire.) The wire used for the present measurements exhibits Kelvin waves often, and their frequencies provide key geometric information.

Frames (b) and (c) of Fig. 1 expand the oscillations visible at the stable circulation levels. The horizontal axis has the same scale in both cases, illustrating clearly that the oscillations at the first pin have a higher frequency. The periods are about 52 seconds for the first pinned level and 101 seconds for the second level. The period repeats to within the uncertainty of about two seconds for all pinning events at the same level.

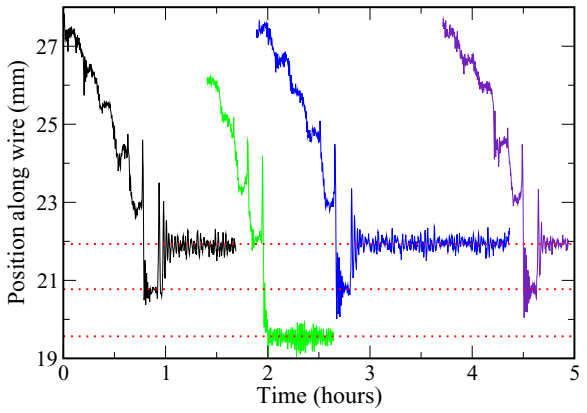


FIG. 2. (Color online) Several approaches of a vortex to the bump, showing the reproducibility of the pin levels. Each curve has an arbitrary horizontal shift.

The Kelvin wave period for long wavelength $\lambda$ is

$$T = \frac{2\lambda^2}{\kappa \ln \frac{\lambda}{2a_o}},$$

where $a_o = 1.3 \times 10^{-7}$ mm is the vortex core radius and $\kappa = 9.97 \times 10^{-2}$ mm$^2$/s is the circulation of a single-quantum vortex [10]. For a pinned vortex, the lowest-frequency mode has a wavelength four times the length of the free vortex segment. For a pin site at the bump apex, the free vortex length is 1.6 mm and the corresponding period is $T = 48$ seconds, very close to the observed value at the middle pin level. A pin site at the edge of the bump, with vortex length equal to the cell radius of 2.9 mm, corresponds to a period of 164 seconds. The weaker agreement here could mean simply that the vortex does not pin precisely at the bump edge, which is hardly surprising since the straight-line path from the center of the cell to the bump edge passes *through* the bump. The observed period of 101 s suggests a vortex length of 2.3 mm. For our bump, this would occur at a distance 1.2 mm from the bump axis, which is quite close to the edge in the lateral direction.

The Kelvin waves at the third pin level have an intermediate period near 62 seconds. This corresponds to a vortex length of 1.76 mm, which would place the pin site 0.97 mm off the axis. Since the glue ran down in this direction when the bump was affixed to the cell wall, this edge does have a more gradual height change, and the observed values for the pin location and Kelvin wave period are plausible.

Figure 2 collects several vortex pinning events. In three cases a vortex pins to the bump apex, then works free spontaneously after about eight minutes and shifts to a site closer to the bump edge. By contrast, the pins at both the top and bottom edges of the bump never come free without deliberate heating on our part to dislodge the vortex. Thus it appears that for this geometry pinning to the bump apex is less stable than pinning closer to the bump edge. Such temporary pinning does not occur in the computational work [7]. One possible reason for the difference is the much lower dissipation in our actual experiment. The computational vortices are far more able to dispose of excess length through Kelvin oscillations and the resulting energy loss; in our experiment, the barely damped oscillations may continue at high amplitude and eventually dislodge the vortex. The lack of a good dissipation mechanism is a more serious issue for the pin site at the bump apex, because of the relatively short distance from the apex to the wire. When a precessing vortex that terminates on the cylindrical wall then pins at the bump apex, it must either dispel a significant amount of energy or maintain its length through bends in its core.

As noted above, both the pin levels and the Kelvin wave periods for each level are highly reproducible, which strongly suggests that vortices repeatedly pin at the same few spots. However, the initial approaches of the vortices are far from identical. Each trace begins with a few cycles of an oscillation with a period of about 10 minutes, corresponding to precession of the free vortex segment. The minima and maxima indicate

particular directions of the free vortex within the cell [11]. The heights of the minima and maxima vary among the traces, showing that the vortices approach the bump along different trajectories. Nonetheless, they still reach the same pin locations. This cannot occur purely from microscopic roughness at the pin site; macroscopic energy considerations must play a role in guiding the vortex towards the site. Similarly, the three vortices that move from the pin site at the bump apex to one at the bump edge trace out different paths. For example, close examination of Fig. 2 shows that in the first trace the vortex returns to the level of the apex on the first oscillation after depinning, in the second it has two oscillations to intermediate levels, and in the third it settles after only a single oscillation.

One unusual energy consideration, from the Gaussian curvature of the surface [12,13], could explain both the existence of multiple pin sites and the macroscopic energetics that guides a vortex between them. Regions of negative Gaussian curvature are predicted to be more favorable for defects than regions of positive curvature. The arguments rely on energetics of two-dimensional systems, and a proposed test in superfluid helium involves a thin layer of superfluid [12]. In three dimensions, surface energy terms are typically much smaller than bulk terms but may still provide an incremental contribution that leads to a metastable pin location.

A Gaussian curvature effect could account for the particularly unexpected location of one of our pin sites. Since the vortex must be perpendicular to the bump at its pin location, any pin site other than the bump apex requires the vortex to curve. For a stable pinned vortex, the velocity field produced by this curvature exactly cancels the applied velocity field. Following this logic, in our experiment we expect the stable pin site to lie towards the bottom edge of the bump. Yet our measurements repeatedly find a vortex pinning near the *top* edge, where the self-induced velocity near the bump augments the applied velocity rather than opposing it. A pinning force, perhaps deriving from the energetics of Gaussian curvature, is needed to retain the vortex at this spot.

Another result from Schwarz's calculations is that if the fluid velocity is low enough for a vortex to pin, then the vortex will do so as long as it moves along a path that passes within about one bump radius of the edge of the bump [7]. The distortion of the velocity field by the bump pulls the vortex inward until it encounters the bump. By contrast, we find that the vortex does not pin unless its path is directed near the center of the bump. The spikes in Fig. 2 in the two or three precession cycles immediately before a vortex pins indicate that a vortex too far off center moves over the surface of the bump without pinning. As the end of the vortex traverses the bump, the length of the free vortex portion shrinks abruptly. To compensate, the length of circulation trapped on the wire increases sharply, causing the spike in our data. On each circuit of the cell the vortex encounters the bump closer to the bump center, with a corresponding increase in the spike's magnitude. Eventually the path lies close enough to the center that the vortex pins.

We suggest a few reasons contributing to the observed nonpinning events. First, even in Schwarz's original work there is an asymmetry depending on the direction that the vortex approaches the pin site [7]. The asymmetry was not remarked on but is visible in Fig. 25 of that paper. It arises from the mutual friction force, which drives the vortex to one side relative to the direction of the superfluid velocity. A vortex beginning on one side of the bump is driven towards it, while a vortex on the other side is driven away. Thus this contribution either assists or opposes the inward pull towards the bump from the bump's distortion of the local velocity field. In our experimental setup, the vortex always approaches from the direction where the friction contribution makes pinning more difficult. Since the friction is extremely small at our low measurement temperatures, the directional asymmetry should be similarly low. The trapping distance should be reduced from what it would be with more friction driving the vortex towards the bump, but this does not explain what happens after a vortex does encounter the bump. A second factor, as we noted when discussing the relative stability at the bump apex and edge, is that the low friction cannot provide the energy dissipation that would enable the vortex to settle at the bump.

A third possibility for why the vortex in our experimental setup sometimes fails to pin is the nonuniform velocity field. We have carried out simulations that support this explanation. Following Schwarz [7], we calculate the behavior of a vortex near a hemisphere on a flat plane, for different applied velocity fields. Our computational geometry involves the region between two planes, at $z = 0$ and $z = 0.002$ cm. Each plane has a hemispherical bump of radius 0.0001 cm, centered on the $z$ axis. We use an immovable straight vortex line as the source of the applied velocity field. Meeting the boundary condition of zero velocity perpendicular to the surface is then straightforward since the code is already set up to solve the boundary value problem for the fluid flows associated with isolated vortices. The flow from a vortex line is also a plausible analog of the $1/r$ velocity field from the central vortex in our physical experiment. We first use a source vortex parallel to the $y$ axis, at $x = 0$ and $z = 0.0005$ cm. A second vortex at height 0.0015 cm maintains symmetry about the midplane. We require constant but not necessarily quantized circulation for the source vortex, so we can vary the applied field in small increments. The nonuniform velocity field dramatically destabilizes the vortex and enables it to traverse the hemisphere without pinning. The test vortex has a metastable configuration terminating on the hemisphere only when the applied velocity field at the bump apex is less than 0.00059 cm/s. The applied field is larger closer to the source vortex, but is still orders of magnitude smaller than the values reached when the distant velocity field is constant. For the fastest applied field that supports a pinned test vortex, its largest contribution along the length of the test vortex is 0.012 cm/s. By contrast, if the applied velocity field is constant far from the bump, the vortex can pin until the applied field is about 0.66 cm/s, corresponding to a flow of about 1 cm/s past the apex. Repeating the calculations for a source vortex the same distance from the bump but in the $z = -x$ plane confirms the destabilizing nature of nonuniform fields. In this case the largest velocity at the bump apex that allows pinning is 0.0052 cm/s, and the highest applied velocity along the test vortex is again 0.012 cm/s.

We now return to the observation that a vortex can pin at either the edge or the apex of a bump. A different geometry provides additional evidence that this is so. We use a cell where the bump is attached not to the side wall but to one of

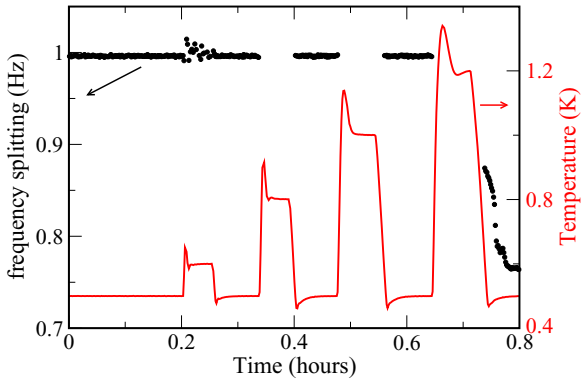


FIG. 3. (Color online) Thermal cycling to depin a vortex from the wire; see text for details. The trace begins with a single quantum of circulation surrounding the entire wire; coincidentally, the frequency splitting for this circulation happens to be very close to 1 Hz.

the endcaps, with the wire glued to the bump apex. Thus a vortex trapped along the entire length of the wire terminates at the apex. Alternatively, a vortex that leaves the wire shortly before it reaches the bump and traverses the superfluid as a free vortex can pin near the edge of the bump. We cannot distinguish these two situations directly. The slight change in beat frequency is unobservably small, particularly because the measurement sensitivity is vastly reduced near the ends of the wire compared to the middle [14].

However, we do observe an indirect signature related to the stability of pinned vortices. Figure 3 illustrates how we test stability. We provide thermal energy by raising the temperature of the cryostat. At the higher temperatures the damping of the vibrating wire is too high to extract the circulation, so after a few minutes we cool the cryostat and check whether the circulation level has changed. If it has not, we heat to a slightly higher temperature, repeating until the vortex depins. After the vortex dislodges, the ensuing precession signal indicates that the vortex now lies along only part of the wire's length, with one end terminating on the cylindrical wall.

Figure 4 shows vortex depinning temperatures for several cells with different endcap configurations. Each point represents a single pinned vortex, with the temperature derived from a heating sequence such as that in Fig. 3. Many of the cells show a large spread of depinning temperatures, possibly because of details of the heating cycles or the interplay between the circulation and the end of the wire. Nonetheless, some patterns emerge, such as the high stability of vortices in the cell with the hemispherical indentation. Three of the eight endcaps have bumps. In those three, but not in any others, the depin temperatures cluster into two groups, which may correspond

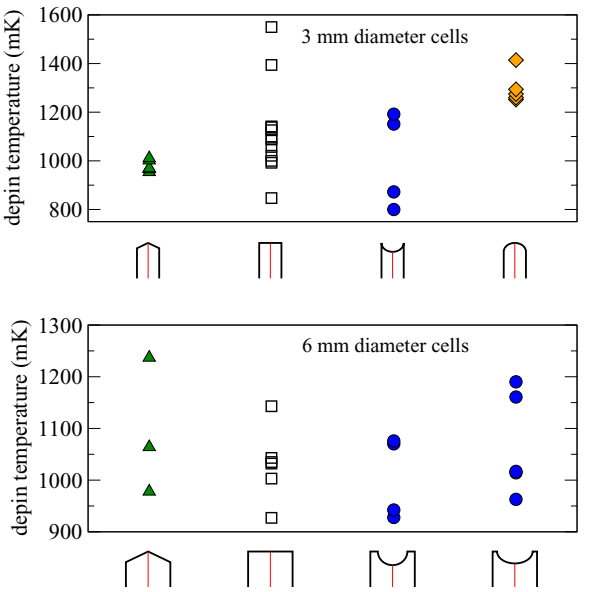


FIG. 4. (Color online) Depin temperatures for eight cells with endcaps as sketched. Each point indicates the maximum temperature reached when a pinned vortex left the wire, e.g., 1.34 K for the vortex of Fig. 3.

to pinning at the bump apex and at the bump edge. A vortex pinned at the bump edge is already close to the outer wall of the cylinder, and we expect it to have a smaller energy barrier to overcome in depinning compared to a vortex that follows the entire wire. Hence the lower-temperature depins for each bump could occur for vortices pinning near the bump edge, while those at higher temperature signify vortices pinning at the apex. We note that the thin cell with a bump has some particularly low depin temperatures and also has the closest approach of the bump edge to the outer wall.

Our measurements agree with the qualitative picture of vortex pinning that arises from numerical simulations. However, given the past successes of superfluid hydrodynamics calculations, the discrepancies may indicate additional physics not accounted for in the computations. We observe multiple metastable pin sites on a single convex bump. In addition, vortices passing near the bump do not spiral inward and pin. On the contrary, even vortices that encounter the bump directly sometimes pass over it without pinning. We suggest that low dissipation and a nonlinear velocity field are responsible for the difficulty in pinning, and that the existence of several allowed pin sites results from an energy term related to the Gaussian curvature of the surface.

We acknowledge funding from UC Davis.

[1] K. W. Schwarz, Phys. Rev. B **47**, 12030 (1993).
[2] L. Hough, L. A. K. Donev, and R. J. Zieve, Phys. Rev. B **65**, 024511 (2001).
[3] R. Hänninen, V. B. Eltsov, A. P. Finne, R. de Graaf, J. Kopu, M. Krusius, and R. E. Solntsev, J. Low Temp. Phys. **155**, 98 (2009).
[4] H. Yano, A. Nishijima, S. Yamamoto, T. Ogawa, Y. Nago, K. Obara, O. Ishikawa, M. Tsubota, and T. Hata, J. Phys.: Conf. Series **400**, 012085 (2012).
[5] S. Zuccher, M. Caliari, A. W. Baggaley, and C. F. Barenghi, Phys. Fluids **24**, 125108 (2012).

[6] M. S. Paoletti, M. E. Fisher, and D. P. Lathrop, Physica D **239**, 1367 (2010).
[7] K. W. Schwarz, Phys. Rev. B **31**, 5782 (1985).
[8] W. F. Vinen, Proc. R. Soc. London A **260**, 218 (1961).
[9] R. J. Zieve, C. M. Frei, and D. L. Wolfson, Phys. Rev. B **86**, 174504 (2012).
[10] R. J. Donnelly, *Quantized Vortices in Helium II* (Cambridge University Press, Cambridge, 1991).
[11] R. J. Zieve, Yu. Mukharsky, J. D. Close, J. C. Davis, and R. E. Packard, Phys. Rev. Lett. **68**, 1327 (1992).
[12] V. Vitelli and A. M. Turner, Phys. Rev. Lett. **93**, 215301 (2004).
[13] V. Vitelli and D. R. Nelson, Phys. Rev. E **70**, 051105 (2004).
[14] S. C. Whitmore and W. Zimmermann, Jr., Phys. Rev. **166**, 181 (1968).